# SPACE CHARGE WAVES IN MISMATCHED BEAMS*

B. R. Poole#, D. T. Blackfield, Y. –J. Chen, J. R. Harris, LLNL, Livermore, CA 94551, U.S.A.
P. G. O'Shea, University of Maryland, College Park, MD 20742, U.S.A.

*Abstract*

Mismatch oscillations resulting from the propagation of space charge waves in intense beams may lead to halo generation, beam loss, and modification of longitudinal beam properties. These oscillations have amplitudes and frequencies different from that of the main beam and are particularly important in machines such as the University of Maryland Electron Ring (UMER), in which the beam dynamics scales to parameters associated with heavy ion fusion drivers. To study these effects, we use the particle in cell code LSP [1] to simulate space charge wave dynamics in an intense electron beam propagating in a smooth focusing channel with 2-D cylindrical symmetry. We examine the evolution of linear and nonlinear density perturbations for both matched and mismatched beams. Comparisons between LSP simulations and numerical models are presented.

## INTRODUCTION

This work was motivated by the observation of space charge waves in UMER with nonlinear properties [2, 3]. Space charge waves can be created by producing a density perturbation on an electron beam upon illuminating the cathode with a short laser pulse, generating additional electrons through photoemission [4]. The evolution of these perturbations can be described by the cold fluid theory [5]. In the beam frame, a density perturbation will evolve into a fast and slow space charge wave propagating in opposite directions without dispersion in the long wavelength limit. For large perturbations, experimental results show discrepancies from the linear theory [2, 3]. The speed of these disturbances on the beam exceeds the wave speed predicted by the linear theory. In addition, there is a noticeable steepening of the leading edges of these waves, indicating shock formation.

The current density in the waves differs from the main beam. Therefore parts of the beam where the waves are present undergo mismatch oscillations, even if the main beam is matched. Through this process the transverse dynamics become coupled to the longitudinal dynamics associated with the waves. Such coupling is of interest because of the connection between mismatch and halo generation [6].

## THEORY AND MODELING

To study these effects, we chose an intense nonrelativistic electron beam similar to that in UMER, but with larger current and simplified focusing. We consider a 10 m long smooth solenoidal focusing channel with a 5 cm radius perfectly conducting beam pipe. The magnetic field is

$$B_z = (B_0/2)(\alpha_- + \alpha_+)\sqrt{4C_2^2/C_1^2}$$
$$\alpha_\pm = \frac{1\pm x}{\sqrt{(1\pm x)^2 + 4C_2^2/C_1^2}} \qquad (1)$$
$$x = 2(z - z_0)/C_1$$

where $z_0 = 10$ m, $C_1 = 19$ m, and $C_2 = 0.05$ m. We adjust $B_0$ to give varying degrees of mismatch. A 10 keV, 207 mA electron beam with negligible emittance is injected into the channel through the fringe field region. This beam is initially converging with $R_{b0} = 4$ cm and $R'_{b0} = -90.4$ mr. The resulting beam and focusing parameters, including the mismatch period $\lambda_e$, are shown in Table 1. The beam envelope can be determined from the transverse envelope equation

$$R''_b + k_0^2 R_b - K/R_b = 0\,, \qquad (2)$$

where the zero-current betatron wavenumber is

$$k_0 = qB_z/2m\beta\gamma c\,, \qquad (3)$$

and the beam perveance is

$$K = (I_{b0}/I_0)(2/\beta^3\gamma^3)\,, \qquad (4)$$

with $I_0 = 17.1$ kA. For our simulations, $K = 3.1\times10^{-3}$.

Table 1: Equilibrium Beam Conditions.

| $B_0$ (G) | $\langle R_b \rangle$ (cm) | $\Delta R_b$ (cm) | $\lambda_e$ (cm) | $\lambda_0 = 2\pi/k_0$ (cm) |
|---|---|---|---|---|
| 36.9 | 1.01 | 0.01 | 80.3 | 115.0 |
| 40.0 | 0.95 | 0.07 | 75.4 | 106.5 |
| 48.0 | 0.80 | 0.21 | 61.8 | 88.7 |

Figure 1 shows LSP results and the solution of the envelope equation with $B_0 = 48$ G for the first 3 m of the focusing channel.

*This work performed under the auspices of the U.S. Department of Energy by Lawrence Livermore National Laboratory under Contract DE-AC52-07NA27344.
#poole1@llnl.gov

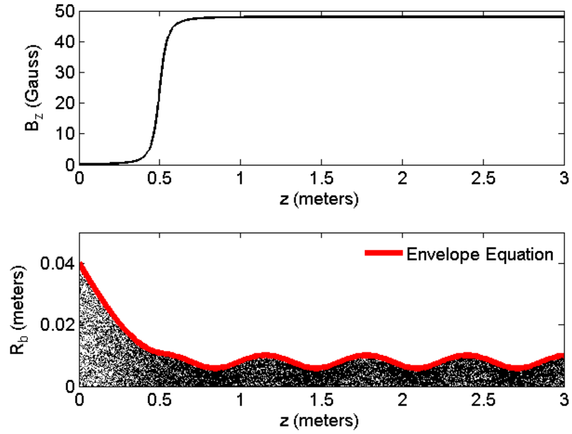


Figure 1: LSP simulation and envelope equation solution for a mismatched beam with $B_0 = 48$ G.

To launch space charge waves after the focusing channel has filled, a density perturbation is introduced at the emission surface. Assuming no energy perturbation, this provides a beam current of the form

$$I_b = I_{b0}\left(1+\delta e^{-(t-t_0)^2/\tau^2}\right), \tag{5}$$

where $I_{b0} = 207$ mA, $t_0 = 237.5$ ns, and $\tau = 5$ ns. The spatial scale of the perturbation is $\beta c\tau = 0.29$ m and the perturbation strengths are $\delta = 0.2$, 0.6, or 1.0.

Figure 2 shows the space charge wave evolution using LSP for $\delta = 0.2$. In the beam frame, the space charge wave speed in this case is $\pm 4.75\times 10^6$ m/s.

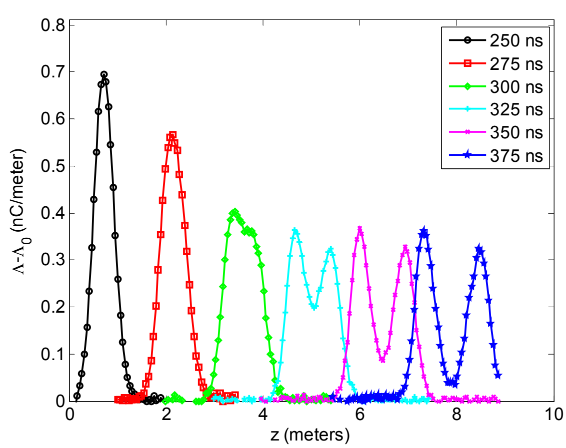


Figure 2: LSP results showing the evolution of slow and fast wave line charge density perturbations for $\delta = 0.2$.

In the long wavelength limit, the nonlinear cold-fluid equations are

$$\frac{\partial \tilde{\Lambda}}{\partial t} + v_0\frac{\partial \tilde{\Lambda}}{\partial z} + \Lambda_0\frac{\partial \tilde{v}}{\partial z} + \frac{\partial}{\partial z}\left(\tilde{\Lambda}\tilde{v}\right) = 0 \tag{6}$$

and

$$\frac{\partial \tilde{v}}{\partial t} + v_0\frac{\partial \tilde{v}}{\partial z} + \tilde{v}\frac{\partial \tilde{v}}{\partial z} = \frac{q}{m\gamma^3}E_z = \frac{-qg}{4\pi\varepsilon_0 m\gamma^5}\frac{\partial \tilde{\Lambda}}{\partial z} \tag{7}$$

where the fluctuating components of the line charge density and velocity are $\tilde{\Lambda} = \Lambda - \Lambda_0$ and $\tilde{v} = v - v_0$. The geometric factor $g$ is $2\ln\left(R_0/R_b\right)$ where the beam and pipe radii are $R_b$ and $R_0$. In the linear regime, this model predicts fast and slow space charge waves propagating in the beam frame with velocities

$$c_0 = \pm\left(qg\Lambda_0/4\pi\varepsilon_0 m\gamma^5\right)^{1/2}. \tag{8}$$

The equilibrium line charge density $\Lambda_0 = I_{b0}/\beta c$ is 3.55 nC/m. The linear space charge wave velocities from Eq. (8) are $\pm 4.05\times 10^6$ m/s. Plots of the fast and slow wave line charge density perturbations at 350 ns using LSP for three perturbation strengths are shown in Fig. 3. Also shown is the numerical solution of Eqs. (6) and (7) for $\delta = 1$.

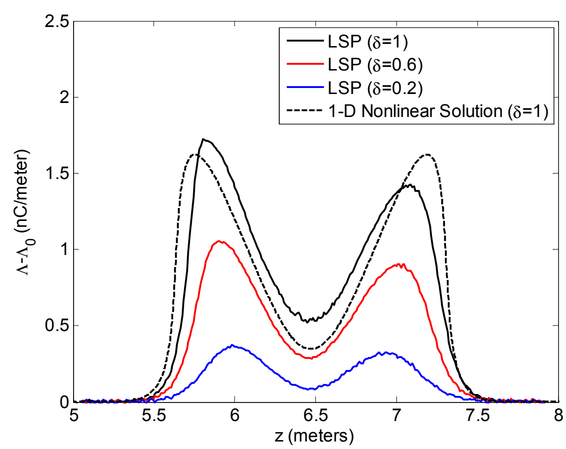


Figure 3: LSP results for a matched beam and solution of nonlinear fluid equations at 350 ns with $B_0 = 36.9$ G.

A shock front is generated at the leading edge of the waves for all simulated perturbation levels. The 1-D nonlinear solution replicates the increase of wave speed with increasing perturbation parameter [3]. However, the solution does not predict the amplitude asymmetry between fast and slow waves observed in the LSP simulations. This asymmetry may be due to the violation of the long wavelength approximation since the scale length of the perturbation is comparable with the beam pipe diameter.

Figure 4 shows LSP results with $\delta = 1$ for matched and mismatched beams with focusing fields of 36.9 G and 48 G.

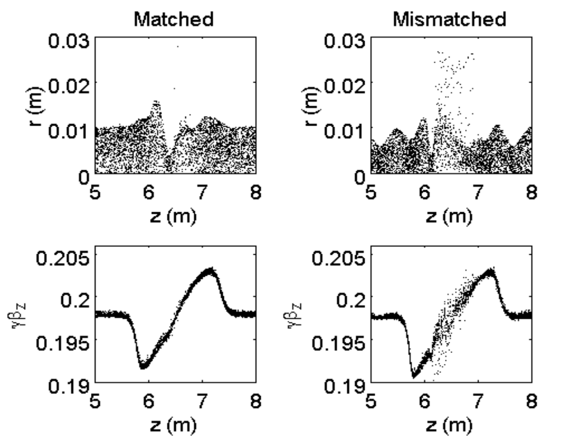


Figure 4: Beam envelope and longitudinal phase space at 350 ns for matched and mismatched beams with $\delta = 1$.

The longitudinal phase space shows the momentum perturbations associated with the fast and slow space charge waves. For the mismatched beam there is additional longitudinal and transverse structure in this region. Figure 5 shows the additional high frequency structure in the line charge density disturbance at 350 ns, for three perturbation strengths.

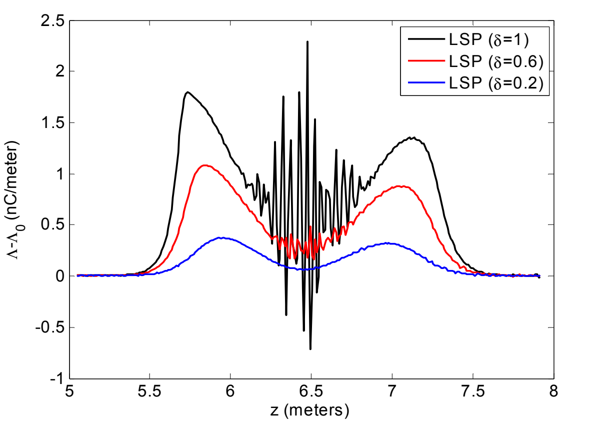


Figure 5: LSP results for mismatched beam at 350 ns with $B_0 = 48$ G.

This high spatial frequency structure appears only for mismatched beams and in the region between the fast and slow waves. The spacing of this structure is about 5 cm, an order of magnitude less than the mismatch wavelength. LSP simulations show ejection of electrons from the beam core by the fast and slow waves near the peak mismatch amplitudes, producing halo and emittance growth as seen in Fig. 6. This suggests a partial explanation of this structure. Ejection events occur each time a wave passes through its mismatch amplitude maximum. The time between these events is $\lambda_e/(\beta c \pm c_w)$ where $\pm c_w$ are the wave velocities in the beam frame. Meanwhile the ejected electrons move at $\beta c$ and are left behind by these waves so the next ejection event occurs at a slightly different location. The distance in the beam frame between these locations is

$$\lambda_h = c_w \lambda_e / (\beta c \pm c_w). \tag{9}$$

Equation (9) predicts that $\lambda_h = 5.6$ cm is a factor of 11 smaller than the mismatch period of $\lambda_e = 61.8$ cm. Assuming particle ejection from both waves, it appears that the number of ejection events, hence the number of longitudinal features seen, should be twice the number of mismatch periods through which the perturbation has passed. This is consistent with LSP.

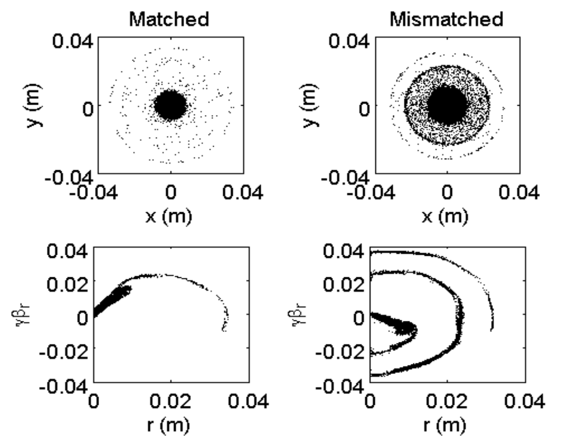


Figure 6: Transverse phase space at 350 ns and 6.5 meters comparing matched and mismatched beams for $\delta = 1$.

## CONCLUSIONS

The dynamics of space charge waves were examined for matched and mismatched beams with weak and strong nonlinear perturbations. Both LSP and numerical solutions of nonlinear fluid equations were used to examine wave dynamics. LSP found shock generation in the leading edge of the space charge waves consistent with the nonlinear fluid model. Amplitude asymmetries between the fast and slow waves were observed using LSP, possibly due to violation of the long wavelength approximation. For a mismatched beam, a large density perturbation produced a short wavelength longitudinal spatial structure along with halo generation and transverse emittance growth.

## REFERENCES


[1] LSP, a product of Voss Scientific, Albuquerque, NM.
[2] J. C. T. Thangaraj, *et al.*, Proc. Advanced Accelerator Concepts, 732 (2008).
[3] J. C. T. Thangaraj, *et al.*, Proc. PAC'07, 3570 (2007).
[4] J. G. Neumann, *et al.*, Rev. Sci Instrum. **76,** 033303 (2005).
[5] J. G. Wang, *et al.*, Phys. Rev. Lett. **71**, 1836 (1993).
[6] R. L. Gluckstern, Phys. Rev. Lett. **73**, 1247 (1994).